LASER &
PHOTONICS
REVIEWS

WILEY-VCH

REPRINT

Laser & Photon. Rev. **3**, No. 1–2, 67–85 (2009) / **DOI** 10.1002/lpor.200810038

**Laser & Photonics
Reviews**

67

Abstract We present an overview of solid-state optical refrigeration also known as laser cooling in solids by fluorescence upconversion. The idea of cooling a solid-state optical material by simply shining a laser beam onto it may sound counter intuitive but is rapidly becoming a promising technology for future cryocoolers. We chart the evolution of this science in rare-earth doped solids and semiconductors.

Measured cooling efficiency as a function of the pump laser wavelength for a 1.2% Tm^{+3} doped BaY_2F_8 crystal at room temperature. The solid line is calculated using the absorption spectrum [30].
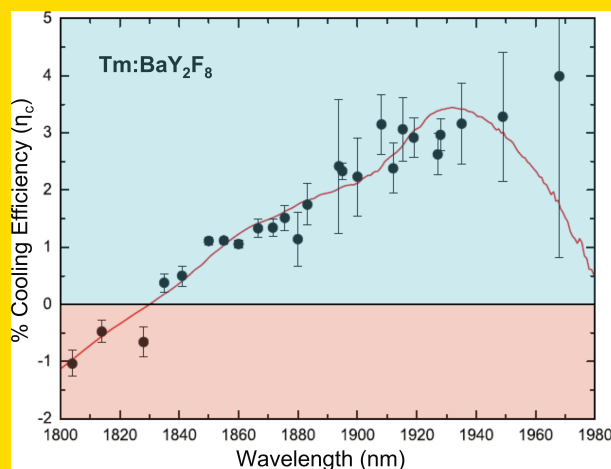
Laser cooling of solids

Mansoor Sheik-Bahae[1,*] *and Richard I. Epstein*[1,2]

[1] Optical Science and Engineering, Department of Physics & Astronomy, University of New Mexico, Albuquerque, NM, USA
[2] Los Alamos National Laboratory, Los Alamos, NM, USA

1. Basic concepts

The term "laser cooling" is most often used in association with cooling and trapping of dilute gases of atoms and ions to extremely low temperatures. This area of science has progressed rapidly in the last two decades and has facilitated the observation of Bose-Einstein condensates and many related phenomena [1, 2]. It is surprising that nearly half a century before Doppler cooling of atoms was ever contemplated and more than thirty years before invention of the laser, German physicist Peter Pringsheim (Fig. 1) proposed cooling of solids by fluorescence up-conversion [3]. In the solid phase, atoms do not possess relative translational motion – their thermal energy is largely contained in the vibrational modes of the lattice. The physics of laser cooling of solids (or optical refrigeration) does have essen-

tial similarities to atom cooling: light quanta in the red tail of the absorption spectrum are absorbed from a monochromatic source followed by spontaneous emission of more energetic (blue-shifted) photons. In the case of solids, the extra energy is extracted from lattice phonons, the quanta of vibrational energy in which heat is contained. The removal of these phonons is equivalent to cooling the solid. This process has also been termed "anti-Stokes fluorescence" and "luminescence up-conversion" cooling.

Laser cooling of solids can be exploited to achieve an all-solid-state cryocooler [4–6] as conceptually depicted in Fig. 2. The advantages of compactness, no vibrations, no moving parts or fluids, high reliability, and no need for cryogenic fluids have motivated intensive research. Space-borne infrared sensors are likely to be the first beneficiaries, with other applications requiring compact cryocooling reap-
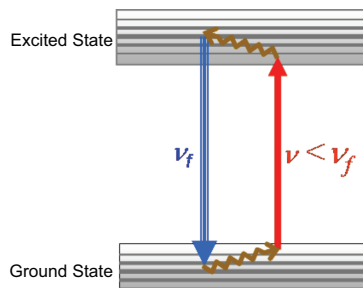
Figure 1 (online color at: www.lpr-journal.org) In 1929, Peter Pringsheim suggested that solids could cool through anti-Stokes fluorescence in which a substance absorbs a photon and then emits one of greater energy. The energy diagram on the right shows one way this could occur. An atom with two broad levels is embedded in a transparent solid. The light source of frequency $h\nu$ excites atoms near the top of the ground state level to the bottom of the excited state. Radiative decays occurring after thermalization emit photons with average energy $h\nu_f > h\nu$.

ing the benefits as the technology progresses. A study by Ball Aerospace Corporation [7] shows that in low-power, space-borne operations, ytterbium-based optical refrigeration could outperform conventional thermoelectric and mechanical coolers in the temperature range between 80–170 K. Efficient, compact semiconductor lasers can pump optical refrigerators. In many potential applications, the requirements on the pump lasers are not very restrictive. The spectral width of the pump light has to be narrow compared to the thermal spread of the fluorescence. Multimode, fiber coupled laser with spectral widths of several nanometers would be adequate. In an optical refrigerator the cooling power is of the order 1 percent of the pump laser power. For micro-cooling applications, with mW heat lift, only modest lasers are adequate. For larger heat lifts, correspondingly more powerful lasers are needed. In all cooling applications, the cooling element has to be connected to the device

being cooled, the *load*, by a thermal link; see Fig. 2. This link siphons heat from the load while preventing the waste fluorescence from hitting the load and heating it.

Another potential application of laser cooling of solids is to eliminate heat production in high-power lasers. Even though laser emission is always accompanied by heat production, Bowman [8,9] realized that in some laser materials, the pump wavelength can be adjusted so that the spontaneous anti-Stokes fluorescence cooling compensates for the laser heating. Such thermally balanced laser would not suffer thermal defocusing or heat damage.

The process of optical refrigeration can occur only in special high purity materials (see section III) that have appropriately spaced energy levels and emit light with high quantum efficiency. To date, optical refrigeration research has been confined to glasses and crystals doped with rare-earth elements and direct-band semiconductors such as gallium arsenide. Laser cooling of rare-earth doped solids have been successfully demonstrated, while observation of net cooling in semiconductors has remained elusive. Fig. 1 schematically depicts the optical refrigeration processes for a two level system with vibrationally broadened ground and excited state manifolds. Photons from a low entropy light source (i.e. a laser) with energy $h\nu$ excite atoms from the top of the ground state to the bottom of the excited-state. The excited atoms reach quasi-equilibrium with the lattice by absorbing phonons. Spontaneous emission (fluorescence) follows with a mean photon energy $h\nu_f$ that is higher than that of the absorbed photon. This process has also been called anti-Stokes fluorescence. There were initial concerns that the second law of thermodynamics might be violated until Landau clarified the issue in 1946 by assigning an entropy to the radiation [10].

In the aforementioned simple model, the interaction rate between electrons and phonons within each manifold is assumed to be far faster than the spontaneous emission rate, which is valid for a broad range of materials and temperatures. The cooling efficiency or fractional cooling
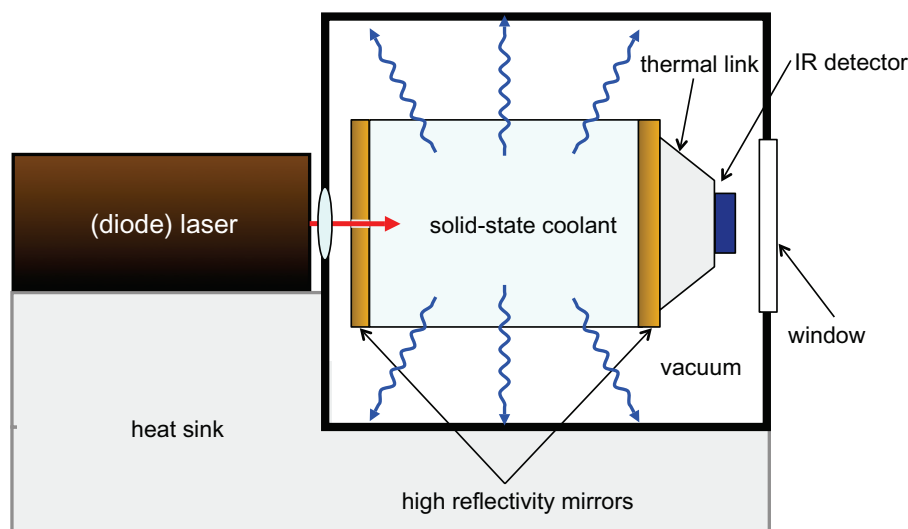
Figure 2 (online color at: www.lpr-journal.org) Schematic of an optical refrigeration system. Pump light is efficiently generated by a semiconductor diode laser. The laser light enters the cooler through a pinhole in one mirror and is trapped by the mirrors until it is absorbed. Isotropic fluorescence escapes the cooler element and is absorbed by the vacuum casing. A sensor or other load is connected in the shadow region of the second mirror. Fig. 2 has been reproduced from [6].

Laser & Photon. Rev. **3**, No. 1–2 (2009)

**Laser & Photonics
Reviews**

69

energy for each photon absorbed is

$$\eta_c = \frac{h\nu_f - h\nu}{h\nu} = \frac{\lambda}{\lambda_f} - 1 \qquad (1a)$$

where $\lambda = c/\nu$ is the wavelength. The invention of the laser in 1960 prompted several unsuccessful attempts to observe laser cooling of solids [11–13]. In 1995, net cooling was first achieved by workers at Los Alamos National Laboratory [14]. Two technical challenges were addressed and overcome in these experiments. The Los Alamos researchers had to have a system in which i) the vast majority of optical excitations recombine radiatively and ii) there is a minimal amount of parasitic heating due to unwanted impurities. Both of these critical engineering issues are ignored in the idealized situation described by Eq. (1a), but are key to experimental success.

It is also important that spontaneously emitted photons escape the cooling material without being trapped and re-absorbed, which would effectively inhibit spontaneous emission [15,16]. This is a critical issue for high index semiconductors where total internal reflection can cause strong radiation trapping. In the absence of radiation trapping, the fraction of atoms that decay to the ground state by the desired radiative process is known as the quantum efficiency, $\eta_q = W_{\rm rad}/(W_{\rm rad} + W_{\rm nr})$ where $W_{\rm rad}$ and $W_{\rm nr}$ are radiative and nonradiative decay rates, respectively. Including a fluorescence escape efficiency η_e defines an external quantum efficiency (EQE): $\eta_{\rm ext} = \eta_e W_{\rm rad}/(\eta_e W_{\rm rad} + W_{\rm nr})$, which assumes the fluorescence is re-absorbed within the excitation volume (see section IV). This describes the efficiency by which a photo-excited atom decays into an escaped fluorescence photon in free space. In a similar fashion, an absorption efficiency $\eta_{\rm abs} = \alpha_r/(\alpha_r + \alpha_b)$ is defined to account for the fraction of pump laser photons that are engaged in cooling [6,17]. Here α_r is the resonant absorption coefficient and α_b is the unwanted parasitic (background) absorption coefficient. As will be derived in sections II and IV, the combination of all these effects re-defines the cooling efficiency as:

$$\eta_c = \eta_{\rm ext}\eta_{\rm abs}\frac{\lambda}{\lambda_f} - 1 \qquad (1b)$$

where the product $\eta_{\rm ext}\eta_{\rm abs}$ indicates the efficiency of converting an absorbed laser photon to an escaped fluorescence photon. Note that $\eta_{\rm abs}$ is frequency-dependent and falls off rapidly below photon energy $h\nu_f - k_B T$ where k_B is the Boltzmann constant and T is the lattice temperature. At pump photon energies much more than $k_B T$ below $h\nu_f$, $\eta_{\rm abs}$ is too small to make $\eta_c > 0$ and laser cooling is unattainable. The above analysis defines the approximate condition needed for laser cooling [6,17].:

$$\eta_{\rm ext}\eta_{\rm abs} > 1 - \frac{k_B T}{h\nu_f} \qquad (2)$$

This relation quantifies the needed efficiencies: cooling a material from room temperature with a nominal energy gap

(pump photon) of 1 eV from room temperature demands that $\eta_{\rm ext}\eta_{\rm abs} > 97\%$. Although suitable lasers were available in the early 1960's, more than three decades of progress in material growth were needed to satisfy this condition.
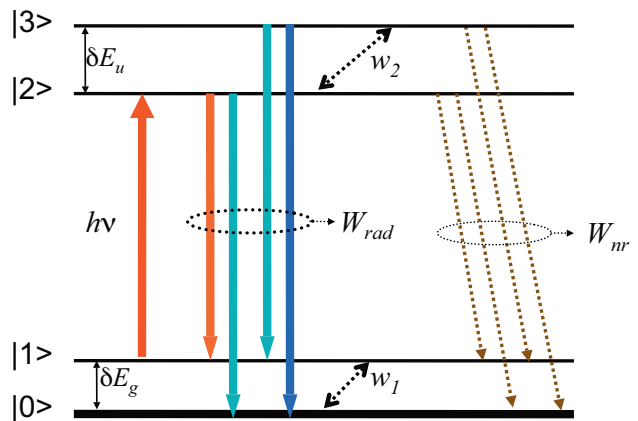
2. The 4-level model for optical refrigeration

Consider the 4-level system of Fig. 3 in which the ground state manifold consist of two closely spaced levels of $|0\rangle$ and $|1\rangle$ with an energy separation $\delta E_{\rm g}$. The excited manifold consists of two states $|3\rangle$ and $|2\rangle$ with an energy separation $\delta E_{\rm u}$. Laser excitation at $h\nu$ is tuned to be in resonance with the $|1\rangle$–$|2\rangle$ transition as shown by the solid red arrow. The double-line arrows depict the spontaneous emission transitions from the upper level to the ground states with a rate of $W_{\rm rad}$; this rate is assumed to be the same for all four transitions. The nonradiative decay rates (indicated by the dotted lines) are also assumed to be equal and given by W_{nr}. The population in each manifold reaches a quasi-thermal equilibrium via an electron-phonon interaction rate given by w_1 and w_2 for lower and upper states, respectively.

The rate equations governing the density populations N_0, N_1, N_2, and N_3 are:

$$\frac{dN_1}{dt} = -\sigma_{12}\left(N_1 - \frac{g_1}{g_2}N_2\right)\frac{I}{h\nu} + \frac{R}{2}\left(N_2 + N_3\right)$$
$$- w_1\left(N_1 - \frac{g_1}{g_0}N_0 e^{-\delta E_g/k_B T}\right), \qquad (3a)$$

$$\frac{dN_2}{dt} = \sigma_{12}\left(N_1 - \frac{g_1}{g_2}N_2\right)\frac{I}{h\nu} - RN_2$$
$$+ w_2\left(N_3 - \frac{g_3}{g_2}N_2 e^{-\delta E_u/k_B T}\right), \qquad (3b)$$

Figure 3 (online color at: www.lpr-journal.org) The four-level energy model for optical refrigeration consisting of two pairs of closely spaced levels: $|0\rangle$ and $|1\rangle$ in the ground state and $|2\rangle$ and $|3\rangle$ in the excited state manifolds.

$$\frac{dN_3}{dt} = -RN_3 - w_2 \left(N_3 - \frac{g_3}{g_2} N_2 e^{-\delta E_u/k_B T} \right) \quad (3c)$$

$$N_0 + N_1 + N_2 + N_3 = N_t \quad (3d)$$

where $R = 2W_{\text{rad}} + 2W_{\text{nr}}$ is the total upper state decay rate, σ_{12} is the absorption cross section associated with $|1\rangle$–$|2\rangle$ transition, I is the incident laser irradiance and the g_i terms represent degeneracy factors for each level . The weighting factor in the electron-phonon interaction terms (w_1 and w_2) maintains the Boltzmann distribution among each manifold at quasi equilibrium. The net power density deposited in the system is the difference between absorbed and out-radiated contributions:

$$
\begin{aligned}
P_{\text{net}} = &\, \sigma_{12} N_1 \left(1 - \frac{g_1 N_2}{g_2 N_1} \right) I \\
&- W_{\text{rad}} \left[N_2 \left(E_{21} + E_{20} \right) + N_3 \left(E_{31} + E_{30} \right) \right] \\
&+ \alpha_b I \,,
\end{aligned}
\quad (4)
$$

where the first term is the laser excitation ($|1\rangle$-$|2\rangle$ transition) and second term includes the spontaneous emission terms from levels $|2\rangle$ and $|3\rangle$ with their respective photon energies. We have also included a term that represents parasitic absorption of the pump laser with an absorption coefficient of α_b. It is straightforward to evaluate the steady-state solution to the above rate equations by setting the time derivatives to zero. To emphasize certain features, we ignore saturation and assume unity degeneracy for all levels. The net power density is then obtained as:

$$P_{\text{net}} = \alpha I \left(1 - \eta_q \frac{h\nu_f}{h\nu} \right) + \alpha_b I, \quad (5)$$

where $\eta_q = (1 + W_{\text{nr}}/W_{\text{rad}})^{-1}$ is the (internal) quantum efficiency and $h\nu_f$ denotes the mean fluorescence energy of the four-level system given by:

$$h\nu_f = h\nu + \frac{\delta E_g}{2} + \frac{\delta E_u}{1 + (1 + R/w_2)e^{\delta E_u/k_B T}} \quad (6)$$

The ground state resonant absorption α is given by:

$$\alpha = \sigma_{12} N_t \left(1 + e^{\delta E_g/k_B T} \right)^{-1} \quad (7)$$

Despite its simplicity, the four level model reveals essential features of solid-state optical refrigeration: First, Eq. (7) exhibits diminishing pump absorption due to thermal depletion of the top ground state at low temperatures, $k_B T < \delta E_g$. This implies that the width of the ground-state manifold (δE_g) must be narrow to achieve cooling at low temperatures with reasonable efficiency. This issue will be revisited when discussing semiconductors in section IV. Second, Eq. (6) shows that the mean fluorescence photon energy is red shifted at low temperatures, which further lowers the cooling efficiency. This shift would be enhanced if the electron-phonon interaction rate (w_2) is smaller than the upper state recombination rate (R). This

means that if $w_2 < R$, decay of the excited state can occur before thermalization with the lattice, which results in no fluorescence upconversion and no cooling [18]. This extreme limit of *cold electron recombination* is an issue for semiconductors at very low temperatures where the electrons interact with the lattice primarily by relatively slow acoustic phonon [15].

Dividing the Eq. (5) by the total absorbed power density $P_{\text{abs}} = (\alpha + \alpha_b)I$ gives the cooling efficiency $\eta_c = -P_{\text{net}}/P_{\text{abs}}$:

$$\eta_c = \eta_q \eta_{\text{abs}} \frac{h\nu_f}{h\nu} - 1, \quad (8)$$

which is similar to Eq. (1.b) not including the luminescence trapping. The most useful feature of the 4-level model is its description of the temperature-dependence of the cooling in a physically transparent manner. As the temperature is lowered, red-shifting of mean fluorescence wavelength combined with the reduction of the resonant absorption reduces the cooling efficiency. At temperature $T = T_m$ the cooling stops (i.e. $\eta_c(T_m) = 0$). This minimum achievable temperature (T_m) can be lowered by reducing the background absorption (higher purity), increasing the quantum efficiency, and enhancing the resonant absorption (e.g. choosing a material with a narrow ground state manifold). The effect of fluorescence trapping and its consequent re-absorption by both resonant and parasitic processes will further diminish the quantum efficiency. We will discuss this in detail when we analyze of laser cooling in semiconductors where total internal reflection leads to substantial trapping.

3. Cooling rare-earth-doped solids.

The advantages of rare-earth (RE) doped solids for laser cooling had been foreseen for decades. Kastler (1950 [11] and Yatsiv (1961 [13] suggested these materials could be used for optical cooling. The key optical transitions in RE-doped ions involve 4f electrons that are shielded by the filled 5s and 6s outer-shells, which limit interactions with the surrounding lattice. Non-radiative decays due to multi-phonon emission are thus suppressed. Hosts with low phonon energy (*e.g.*, fluoride crystals and glasses) further diminish non-radiative decay and hence boost quantum efficiency. In 1968, Kushida and Geusic [12] attempted to cool a Nd^{3+}:YAG crystal with 1064 nm laser radiation. They reported a reduction of heating, but no cooling; it is unclear whether they observed any anti-Stokes cooling effects. Laser cooling of a solid was first experimentally demonstrated in 1995 with the ytterbium-doped fluorozirconate glass ZBLANP:Yb^{3+} [14]. Laser-induced cooling has since been observed in a range of glasses and crystals doped with Yb^{3+} (ZBLANP [19–22], ZBLAN [23, 24], CNBZn [9, 25] BIG [25, 26], $KGd(WO_4)_2$ [9], $KY(WO_4)_2$ [9], YAG [27], $Y_2 SiO_5$ [27], $KPb_2 Cl_5$ [25, 28], $BaY_2 F_8$ [29–31], and YLF [32, 33]).

Fig. 4 shows the cooling and heating of a sample of Yb^{3+} doped ZBLANP for a range of pump wavelengths [5].

Laser & Photon. Rev. **3**, No. 1–2 (2009)

Laser & Photonics
Reviews

71
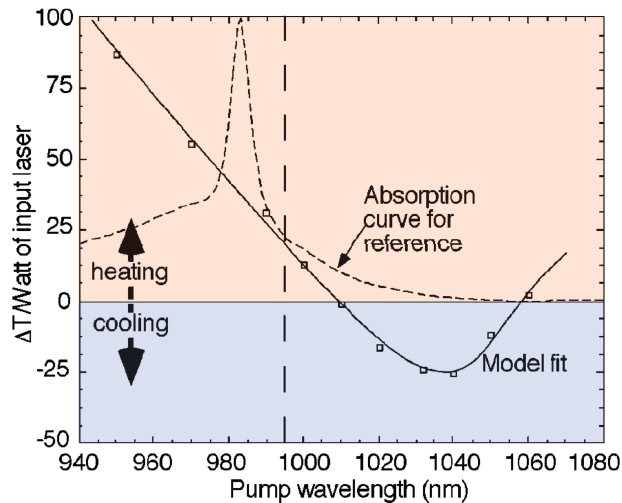
Figure 4 (online color at: www.lpr-journal.org) The temperature change (normalized to incident power) in ytterbium-doped ZBLANP glass as a function of pump wavelength. When the pump wavelength is considerably longer that the mean wavelength of the fluorescence λ_F (vertical dashed line), the escaping light carries more energy than the absorbed laser light and the glass cools. Heating at wavelengths greater than λ_F is due to imperfect quantum efficiency of the fluorescence and non-resonant light absorption [5].

For wavelengths shorter than the mean fluorescence wavelength λ_F (vertical dashed line) the sample heats because of the Stokes shift as well as by non-radiative processes. At longer wavelengths, anti-Stokes cooling dominates and cooling as large as 25 K per watt of absorbed laser power is measured. At still longer wavelengths, absorption by impurities or imperfections dominates, and the sample heats.

In 2000, laser cooling in Tm^{3+} doped ZBLANP was reported at $\lambda \sim 1.9\,\mu m$ [34]. The significance of this result was two-fold: First, it verified the scaling law of Eq. (1.a,b) by demonstrating nearly a factor of two enhancement in the cooling efficiency compared to Yb-doped systems., The enhancement scales as the ratio of the corresponding cooling transition wavelengths. Second, it was the first demonstration of laser cooling in the presence of excited state absorption. A record cooling power of $\sim 73\,mW$ was obtained in this material by employing a multipass geometry [35]. More recently, cooling of Er^{3+} doped glass (CNBZn) and crystal ($KPb_2 Cl_5$) at $\lambda \sim 0.870\,\mu m$ were reported by a Spanish group [36]. It is interesting to note that the cooling transition used in these experiments is between the ground state and the fourth excited state ($^4I_{9/2}$) of Er^{3+}, not the first excited state as illustrated in Fig. 1. High-energy transitions have lower cooling efficiency (Eq. 1) but potentially higher quantum efficiency due to their low nonradiative decay rates to the ground state. The presence of higher excited states in Er^{3+} may prove advantageous since the energy upconversion transitions (i.e. at the cooling wavelengths of the main transition) are endothermic with a high quan-

tum efficiency [36, 37]. This is also the case with cooling of Tm^{3+} [34],

The initial proof-of-principle experiments in ZBLANP:Yb^{3+} achieved cooling by an amount 0.3 K below ambient temperature [14]. The LANL group has since cooled ZBLANP:Yb^{3+} to 208 K starting from room temperature [22] as shown in Fig. 5. Although progress is being made, optical refrigerators need to be more efficient and operate at lower temperatures, below about 170 K, to be competitive with other solid-state coolers such as thermoelectric (Peltier) devices. Several studies have shown that ytterbium- or thulium-doped solids should be capable of providing efficient cooling at temperatures well below 100 K [4, 27, 38].
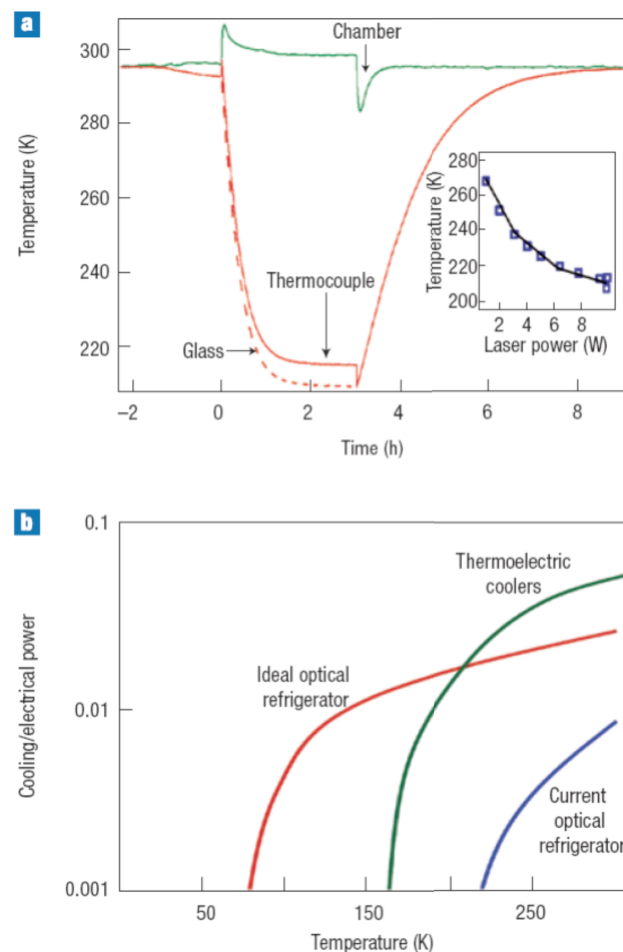
Figure 5 (online color at: www.lpr-journal.org) Panel (a) shows record cooling to 208 K with ZBLANP:Yb^{3+}. The temperatures are measured with thermocouples on the sample and chamber; the internal temperature of the glass is inferred [22]. Panel (b) compares the cooling efficiencies of available thermoelectric coolers (TECs) with ZBLANP:Yb^{3+}-based optical refrigerators. Devices based on materials with low parasitic heating will outperform TECs below 200 . Coolers made from current materials are less efficient than TECs at all temperatures [39]. Fig. 5 (a) has been reproduced from [22]
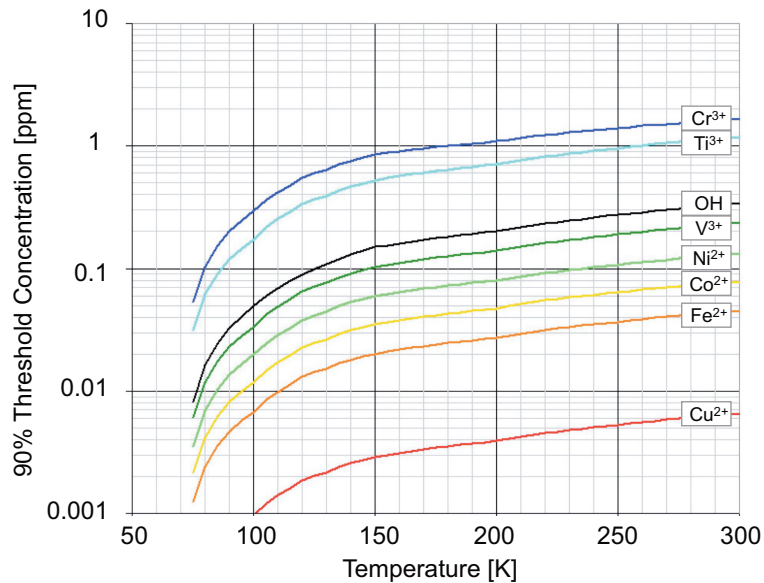
Figure 6 (online color at: www.lpr-journal.org) Calculated impurity threshold concentrations. If the impurity levels of an ion is above the level shown here, the cooling efficiency of the ZBLAN:1%Yb^{3+} will be less than 90% of its ideal value and rapidly converted into heat. See the detailed study by Hehlen et al. [39].

There are several factors that limit the cooling of rare-earth-doped solids in available materials. The most significant factor is the choice of laser cooling medium. The ideal cooling efficiency (Eq. 1) shows that there is an advantage of pumping with lower energy photons. This increased efficiency was part of the motivation for investigating thulium-doped cooling materials, since their ground- and excited state manifolds are separated by about 0.6 eV compared to 1.2 eV in ytterbium-doped solids. There are obstacles, however, in going to longer wavelengths. First is the more limited choices of pump lasers since there are fewer available near 0.6 eV than near 1.2 eV. While not a fundamental consideration, it needs to be kept in mind for near-term commercialization. A second and more general reason involves the ratio of radiative to non-radiative relaxation decays. The rate of non-radiative, heat-producing, multi-phonon decay decreases exponentially with the separation between the ground- and first excited-state manifolds; this is the well-know energy-gap law. In practical terms, this means that because of the relatively large energy of the excited level in ytterbium-doped materials, non-radiative decays do not significantly decrease the quantum efficiency. For pure thulium-doped material, non-radiative decay can overwhelm anti-Stokes cooling, depending on the properties of the host material. For materials with low maximum phonon energies, such as ZBLANP and other fluoride hosts, the non-radiative decays are relatively slow. Many thulium-doped oxide crystals and glasses have rapid nonradiative decay rates that prevent laser cooling.

Another consideration in the choice of cooling medium is the width of the ground state manifold. According to Boltzmann statistics, lower energy levels in the manifold are more populated than higher ones. As the temperature falls and $k_B T$ becomes small compared to the energy width of the ground-state manifold, the upper levels become depopulated leading to increased transparency at lower fre-

quencies; this effect is illustrated in the four-level system discussed above. The net effect is that at low temperatures the numerator of Eq. (2) becomes small and cooling efficiency goes to zero; see Eq. (1b). The width of the ground state manifold is typically the result of crystal field splitting and depends on both the dopant ion and the host material. By choosing ions and a host that give narrow ground-state manifolds, the material can cool to lower temperatures before the low-frequency transparency condition sets in.

For the material systems studied so far, cooling is not limited by the reasons outlined above. It is most likely hindered by parasitic heating in the bulk of the cooling material or on its surface. As one can see in Fig. 5b, the cooling efficiencies of currently available ZBLANP:Yb^{3+} are far below that for an ideal material with no parasitic heating. One important source of heating in this material is quenching of excited ytterbium ions by impurities such as iron and copper. The radiative decay time of an excited Yb^{3+} ion is about 1 ms. During this time, the excitation migrates through the glass by transferring energy to neighboring ions. If the excitation encounters an impurity atom, the energy can be transferred to this atom and rapidly converted into heat. A detailed study by Hehlen et al. [39] found that the ideal cooling efficiency can be approached when concentration of impurities such as Cu^{2+} is less than 0.01 ppm and that for Fe^{2+} is below 0.1 ppm; see Fig. 6.

An additional source of parasitic heating is absorption in the mirrors that trap the pump radiation in the cooling element. In the LANL experiments, the cooling glass has a pair of high-reflectivity mirrors deposited on two surfaces, as depicted in Fig. 2. Pump light is reflected multiple times by each mirror, so that that even relatively low absorption of 0.0001 per surface produces significant heating. Depositing higher quality dielectric mirror may obviate this problem. An alternative approach is to avoid dielectric mirrors all together and exploit the total-internal refection inside the

Laser & Photon. Rev. **3**, No. 1–2 (2009)

**Laser & Photonics
Reviews**

73
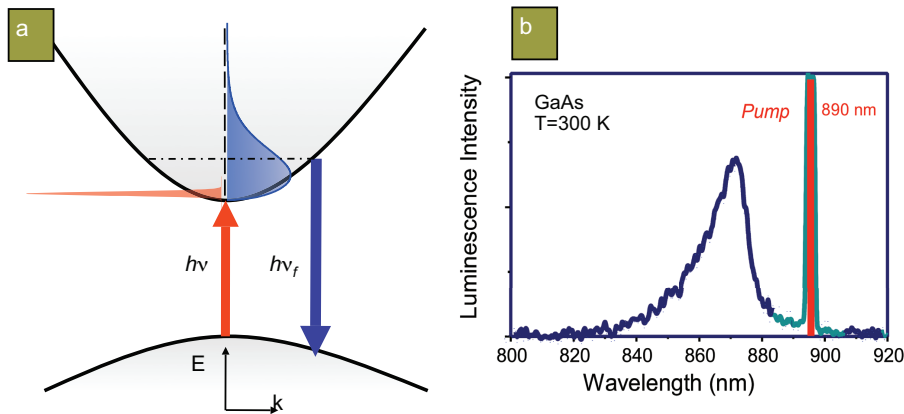
Figure 7 (online color at: www.lpr-journal.org) (a) Cooling cycle in laser refrigeration of a semiconductor in which absorption of laser photons with energy $h\nu$ creates a cold distribution of electron-hole carriers (only electron distribution is shown for clarity). The carriers then heat up by absorbing phonons followed by an up-converted luminescence at $h\nu_F$. (b) Typical anti-Stokes luminescence observed in GaAs/GaInP double heterostructure [6].

cooling medium for circulating the pump beam [40]. Another method of enhancing pump absorption is using resonant cavity effects. Both intra-laser-cavity [24] and external resonant-cavity [41] geometries have been demonstrated. The latter approach has been capable of achieving pump absorption exceeding 90% [41]. Most recently, using active stabilization, this method was employed to achieve $\Delta T \approx 70\,\text{K}$ in a Yb:YLF crystal [33]. This is a highly promising result considering that it was obtained with full black-body thermal load which is nearly 5 times higher than that reported in [22]. It has also been proposed that photon localization in nanocrystalline powders can be exploited to enhance laser pump absorption in cooling of rare-earth doped systems [42].

4. Prospects for laser cooling in semiconductors

Researchers have examined other condensed matter systems beyond RE-doped materials, with an emphasis on semiconductors [17, 43–46]. Semiconductor coolers provide more efficient pump light absorption, the potential of much lower temperatures, and the opportunity for direct integration into electronic and photonic devices. These materials provide their own set of engineering challenges, however, and no net cooling has been observed yet. The essential difference between semiconductors and RE-doped materials is in their cooling cycles. In the latter, the cooling transition occurs in localized donor ions within the host material while the former involves transition between extended valence and conduction bands of a direct gap semiconductor (see Fig. 7a). Indistinguishable charge carriers in Fermi-Dirac distributions may allow semiconductors to get much colder than RE materials. The highest energy levels of the ground state manifold in the RE-doped systems become less populated as the temperature is lowered, due to Boltzmann statistics. The cooling cycle becomes ineffective when the Boltzmann constant times the lattice temperature becomes comparable to the width of the ground state (see previous section describing the 4-level model). This sets a limit of $T \sim 100\,\text{K}$ for most existing RE-doped systems.

No such limitation exists in pure (undoped) semiconductors – temperatures as low as 10 K may be achievable [47].

Semiconductors should achieve higher cooling power density compared to RE-materials. The maximum cooling power density (rate of heat removal) is $\approx N \times k_B T / \tau_r$, where N is the photo-excited electron (-hole) density and τ_r is the radiative recombination time. In semiconductors the optimal density N is limited due to many-body processes and does not exceed that of moderately doped RE systems. We can gain 5–6 orders of magnitude in cooling power density because the radiative recombination rates in semiconductors are much faster than in RE ions.

Laser cooling of semiconductors has been examined theoretically [15, 44, 45, 47–52] as well as in experimental studies [46, 53–56]. A feasibility study by the authors outlined the conditions for net cooling based on fundamental material properties and light management [15]. Researchers at the University of Arizona [47, 50] studied luminescence upconversion in the presence of partially ionized excitons, which must be understood to attain temperatures approaching 10 K. The role of bandtail states [52], the possible enhancement of laser cooling by including the effects of photon density of states as well as novel luminescence coupling schemes based on surface plasmon polaritons [57, 58] were recently introduced by Khurgin at Johns Hopkins University. Here, we expand on the basic model of [15] and present the theoretical foundation of laser cooling in semiconductor structures with an arbitrary external efficiency. This treatment accounts for the luminescence red-shift due to re-absorption, the effect parasitic absorption of the pump, luminescence power, and band-blocking effects. We then discuss the latest experimental results attempting to make the first observation of laser cooling in a semiconductor material.

We consider an intrinsic (undoped) semiconductor system uniformly irradiated with a laser light at photon energy $h\nu$. Furthermore, we assume that only a fraction η_e of the total luminescence can escape the material while the remaining fraction $(1-\eta_e)$ is trapped and re-cycled, thus contributing to carrier generation. For now, we will ignore the parasitic absorption of luminescence but will later consider its implications. For a given temperature, the rate equations

for the electron-hole pair density (N) is given by [15]:

$$\frac{dN}{dt} = \frac{\alpha I}{h\nu} - AN - BN^2 - CN^3 + (1-\eta_e)BN^2 \quad (9)$$

Here $\alpha(\nu,N)$ is the interband absorption coefficient that includes many-body and blocking factors. The recombination process consists of nonradiative (AN), radiative (BN^2), and Auger (CN^3) rates. All the above coefficients are temperature dependent. The last term represents the increase in N from the re-absorption of the luminescence that does not escape, assuming the re-absorption occurs within the laser excitation volume. The density-dependence of α results from both Coulomb screening and band-blocking (saturation) effects. The latter can be approximated by a blocking factor such that [59,60]:

$$\alpha_(N, h\nu) = \alpha_0(N, h\nu)\{f_v - f_c\}, \quad (10)$$

where α_0 denotes the unsaturated absorption coefficient. The strongly density-dependent blocking factor in the brackets [61] contains Fermi-Dirac distribution functions for the valence (f_v) and conduction (f_c) bands.

Under steady-state conditions, Eq. (9) can be rewritten as

$$0 = \frac{\alpha(\nu, N)}{h\nu}I - AN - \eta_e BN^2 - CN^3. \quad (11)$$

This indicates that the fluorescence trapping effectively inhibits the spontaneous emission as it appears through η_eB only. This result has also been shown previously by Asbeck [16]. It is important to note that η_e is itself an averaged quantity over the entire luminescence spectrum.

$$\eta_e = \frac{\int S(\nu)R(\nu)d\nu}{\int R(\nu)d\nu}. \quad (12)$$

Here $S(\nu)$ is the geometry-dependent escape probability of photons with energy $h\nu$ and $R(\nu)$ is the luminescence spectral density that is related to the absorption coefficient through reciprocity using a "non-equilibrium" van Roosbroeck-Shockley relation (also known as Kubo-Martin-Schwinger (KMS) relation [59,62]:

$$R(\nu, N) = \frac{8\pi n^2 \nu^2}{c^2}\alpha_(\nu, N)\left\{\frac{f_c(1-f_v)}{f_v - f_c}\right\}, \quad (13)$$

where c is the speed of light and n is the index of refraction. Note that the radiative recombination coefficient B is obtained by $BN^2 = \int R(\nu)d\nu$ which results in a negligible dependence of B on N at the carrier densities of interest. The net power density that is deposited in the semiconductor is the difference between the power absorbed from the laser (P_{abs}) and that of the luminescence that escapes (P_{le}):

$$P_{net} = P_{abs} - P_{le} = [\alpha I + \Delta P] - [\eta_e BN^2 h\tilde{\nu}_f], \quad (14)$$

where the absorbed power density includes the resonant absorption (αI) and a term ΔP that accounts for the undesirable effects such as free-carrier absorption and other parasitic absorptive processes. The second term is the escaped luminescence power density at a mean luminescence energy $h\tilde{\nu}_f$ defined as

$$h\tilde{\nu}_f = \frac{\int S(\nu)R(\nu)h\nu d\nu}{\int S(\nu)R(\nu)d\nu}. \quad (15)$$

Note that the escaped mean luminescence energy can deviate (i.e. redshift) from its internal value (S=1) depending on the thickness or photon recycling conditions. With the aid of Eq. (9), we rewrite Eq. (14) as:

$$P_{net} = \eta_e BN^2(h\nu - h\tilde{\nu}_f) + ANh\nu$$
$$+ CN^3 h\nu + \Delta P. \quad (16)$$

Eq. (16) rigorously describes laser cooling of a semiconductor in a compact and simple form. It accounts for the practical considerations of luminescence trapping by introducing an inhibited radiative recombination ($\eta_e B$) and a shifted mean photon energy $h\tilde{\nu}_f$ for the escaped luminescence. For high external efficiency systems where $S(\nu) = 1$, Eq. (16) approaches that described in the literature with $\eta_e = 1$ and $\tilde{\nu}_f = \nu_f$ with ν_f denoting the mean fluorescence energy produced internally in the semiconductor [44–46]. Eq. (16) indicates that laser cooling occurs when $P_{net} < 0$, requiring a dominant contribution from the radiative recombination with $h\nu < h\tilde{\nu}_f$. The cooling efficiency η_c is defined as the ratio of cooling power density P_c ($= -P_{net}$) to the absorbed laser power density ($P_{abs} = \alpha I + \Delta P$). With the aid of Eq. (11), this efficiency can be expressed as

$$\eta_c = -\frac{\eta_e BN^2(h\nu - h\tilde{\nu}_f) + ANh\nu + CN^3 h\nu + \Delta P}{\eta_e BN^2 h\nu + ANh\nu + CN^3 h\nu + \Delta P}. \quad (17)$$

Ignoring the ΔP contributions for the moment, η_c can be written more simply as:

$$\eta_c = \eta_{ext}\frac{\tilde{\nu}_f}{\nu} - 1, \quad (18)$$

where η_{ext} describes the *external* quantum efficiency (or EQE):

$$\eta_{ext} = \frac{\eta_e BN^2}{AN + \eta_e BN^2 + CN^3} \approx (\eta_q)^{1/\eta_e}, \quad (19)$$

with $\eta_q = BN^2/(AN + BN^2 + CN^3)$ denoting the *internal* quantum efficiency [46,63] as also defined more generally following Eq. (5). The approximate equality in Eq. (19) is valid only for η_{ext} near unity (> 0.9). One simple consequence of Eq. (19) is that there is an optimum carrier density $N_{op} = (A/C)^{1/2}$ at which η_{ext} reaches a maximum:

$$\eta_{ext}^{max} = 1 - \frac{2\sqrt{AC}}{\eta_e B} \quad (20)$$

Including background parasitic absorption ($\Delta P = \alpha_b I$), results in more general form of cooling efficiency:

$$\eta_c = \eta_{abs}\eta_{ext}\frac{\tilde{\nu}_f}{\nu} - 1, \quad (21)$$

Laser & Photon. Rev. 3, No. 1–2 (2009)

Laser & Photonics Reviews

75

where the absorption efficiency η_{abs} is the fraction of the total absorbed photons from the pump laser that is consumed by the resonant absorption in the cooling region:

$$\eta_{\mathrm{abs}} = \frac{\alpha(\nu)}{\alpha(\nu) + \alpha_b}, \tag{22}$$

and α_b is assumed to be constant in the vicinity of the band-edge region.

If the pump laser suffers parasitic absorption, so will the luminescence since their frequencies are very close. We now examine the parasitic absorption problem and its effect on the cooling efficiency by revisiting Eq. (9). A small fraction ε_f of the trapped luminescence is absorbed parasitically and the remaining part $(1-\varepsilon_f)$ is recycled through interband absorption thus contributing to the carrier generation. Eq. (9) is rewritten as:

$$\frac{dN}{dt} = \frac{\alpha I}{h\nu} - AN - BN^2 - CN^3 + (1-\eta_e)(1-\varepsilon_f)BN^2. \tag{23}$$

Note that $1 - \varepsilon_f = \bar{\alpha}_f/(\bar{\alpha}_f + \alpha_b) \approx 1 - \alpha_b/\bar{\alpha}_f$ where $\bar{\alpha}_f(\approx \alpha(\nu_f))$ is the interband absorption of the luminescence averaged over its spectrum. Following the same analysis leading to Eq. (21), we obtain the modified cooling efficiency:

$$\eta_c = \bar{\eta}_{\mathrm{ext}}\eta_{\mathrm{abs}}\frac{\bar{\nu}_f}{\nu} - 1, \tag{24}$$

with a modified EQE ($\bar{\eta}_{\mathrm{ext}}$) that is reduced from its ideal value in the high purity ($\alpha_b \approx 0$) approximation to:

$$\bar{\eta}_{\mathrm{ext}} = \eta_{\mathrm{ext}}\frac{1}{1 + \eta_{\mathrm{ext}}\varepsilon_f(1-\eta_e)/\eta_e}$$

$$\simeq \eta_{\mathrm{ext}} - \eta_{\mathrm{ext}}^2\varepsilon_f(1-\eta_e)/\eta_e. \tag{25}$$

This expression is useful for setting an upper bound on the existing intrinsic background absorption of GaAs/InGaP heterostructures. This will be discussed in detail below. Parasitic luminescence absorption is not important in the analysis of photo-carrier density and incident laser irradiance so it is ignored for the moment.

The roots of Eq. (16) define the carrier density range within which net cooling can be observed provided that $\eta_e B(h\tilde{\nu}_f - h\nu) \geqslant 2h\nu\sqrt{AC}$. The equality defines the break-even condition: heating and cooling are in exact balance. At high quantum efficiency, radiative recombination dominates (i.e. $\eta_e B/C \gg N \gg A/\eta_e B$) allowing one to obtain the corresponding laser irradiance from Eq. (11) with the assumption of no band-blocking. We can account for parasitic absorption of the pump by taking $\Delta P = \alpha_b I + \sigma_{\mathrm{fca}}NI$ where α_b denotes an *effective* background parasitic absorption and σ_{fca} is the free-carrier-absorption cross section. In this case, net cooling can occur within an irradiance range of $I_1 < I < I_2$ where $I_{1,2} = (h\nu\eta_e B/\alpha(\nu))N_{1,2}^2$ and

$$N_{1,2} = \left(\frac{h\tilde{\nu}_f - h\nu}{h\nu} - \frac{\alpha_b}{\alpha(\nu)}\right)\frac{\eta_e B}{2C'}\left(1 \mp \sqrt{1 - \frac{A}{A_0}}\right). \tag{26}$$
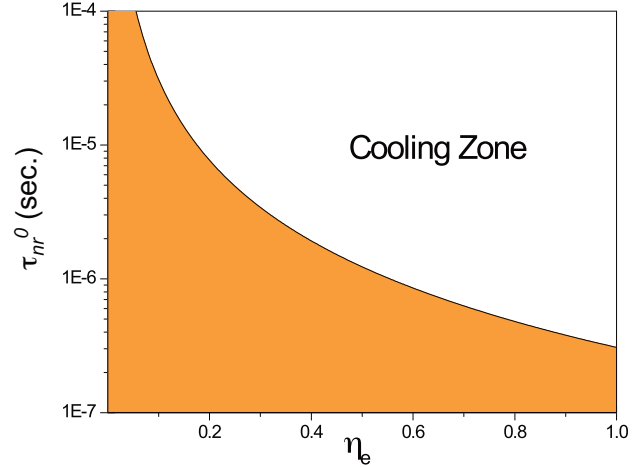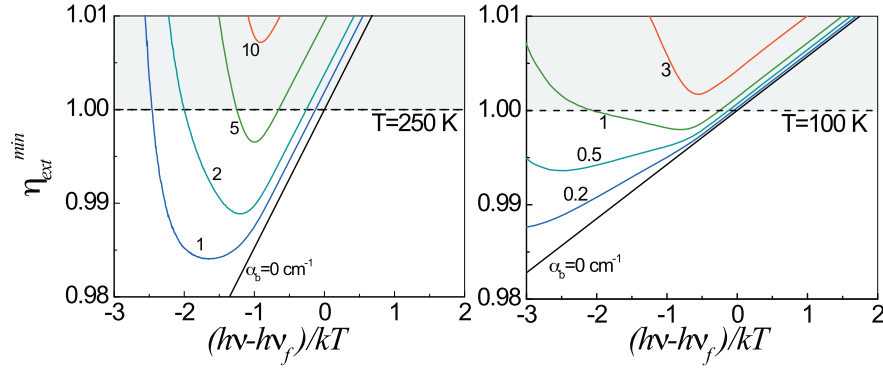

Figure 8 (online color at: www.lpr-journal.org) The break-even nonradiative lifetime as a function of the luminescence extraction efficiency in bulk GaAs calculated using typical values of radiative and Auger recombination at room temperature.

Here $C' = C + \sigma_{\mathrm{fca}}\eta_e B/\alpha(\nu)$, and

$$A_0 = \left(\frac{h\tilde{\nu}_f - h\nu}{h\nu} - \frac{\alpha_b}{\alpha(\nu)}\right)^2\frac{(\eta_e B)^2}{4C'} \tag{27}$$

is the break-even (maximum allowable) nonradiative decay rate for a given excitation energy $h\nu$. Free carrier absorption appears as an enhancement of the Auger process. The parameters B and C are fundamental properties of a semiconductor and have been calculated and measured extensively for various bulk and quantum-confined structures [59, 60, 63, 64] The reported values for these coefficients, however, vary considerably. In bulk GaAs, for example, the published values are $2 \times 10^{-16} < B < 7 \times 10^{-16}$ m³/s and $1 \times 10^{-42} < C < 7 \times 10^{-42}$ m⁶/s [64]. These variations are primarily due to experimental uncertainties. We assume average values of $B = 4 \times 10^{-16}$ m³/s and $C = 4 \times 10^{-42}$ m⁶/s, while ignoring the effects of background and free carrier absorption. These assumptions allow us to gain insight into the feasibility and requirements for achieving net laser cooling. It should be noted that the theoretical values for these parameters, for different models vary almost within the same range as the experimental results. For the simple two-band model used here, $B \approx 5 \times 10^{-16}$ m³/s [65].

Using Eq. (27), we plot in Fig. 8 the break-even nonradiative lifetime $\tau_{\mathrm{nr}}^0 = A_0^{-1}$ as a function of η_e assuming $h\nu_f - h\nu = k_B T$ with $h\nu_f$ corresponding to $\lambda_f \approx 860$ nm at room temperature. The orange area under the curve is the unwanted (heating) zone. Eq. (27) also suggests that increasing the quantum efficiency η_q by decreasing the incident photon energy (e.g. at $h\nu_f - h\nu > k_B T$) relaxes this requirement. Interband absorption drops rapidly as the excitation moves further in the Urbach tail and one may no longer ignore background and free carrier absorption. Recently, it was found that free carrier absorption (FCA) at

Figure 9 (online color at: www.lpr-journal.org) The minimum EQE required to achieve laser cooling versus the normalized excitation photon energy for GaAs at T=250 and 100 K obtained from the inequality of Eq. (29). The absorption data $\alpha(\nu)$ were obtained by using the KMS relations on the PL spectra on a high quality GaAs/InGaP double heterostructures. Note that for certain background absorption α_b, the requirement $\eta_{ext} > 1$ is unattainable (unphysical) for any wavelength. This restriction becomes more prevalent at lower temperature.

the band edge wavelengths is much smaller than previously expected [66, 67]. For GaAs, $\sigma_{FCA} \approx 10^{-24}$ m^2 [66, 67], which requires $\alpha(\nu) \geqslant 10^3$ m^{-1} to ensure that free carrier losses are negligible (i.e. $C' \approx C$). This requirement is satisfied even at $\lambda = 890 \, nm$ (corresponding to $h\nu_f - h\nu \approx 2k_B T$) where $\alpha(\nu) \approx 10^4$ m^{-1}. We conclude that FCA does not pose a limitation on laser cooling.

We can categorize the possible sources and locations of the parasitic background absorption α_b into three regions: (a) active or core material, (b) cladding layers of the heterostructure, and (c) the substrate. It is also implicit that α_b in Eq. (27) is scaled such that for cases (b) and (c), the actual background absorption coefficient $\alpha'_b = \alpha_b \times (d/L)$, where d and L are the thicknesses of the loss and active media (if different) respectively.

While situations (b) and (c) can be controlled experimentally by varying the barrier thickness or using high purity substrate respectively, the parasitic absorption from the cooling layer itself presents the most difficult engineering obstacle. This limitation is revisited in the next section where experiments on laser cooling with GaAs will be analyzed.

It is also instructive to show an alternative and compact way of expressing the cooling condition. With laser excitation at $h\nu < h\bar{\nu}_f$, the cooling condition defined by EQE reduces to:

$$\eta_{ext} > \frac{\nu}{\bar{\nu}_f} + \frac{\alpha_b}{\alpha(\nu)} . \qquad (28)$$

Including the parasitic absorption of luminescence lets us replace η_{ext} by $\bar{\eta}_{ext}$ using Eq. (28) to give a more general condition
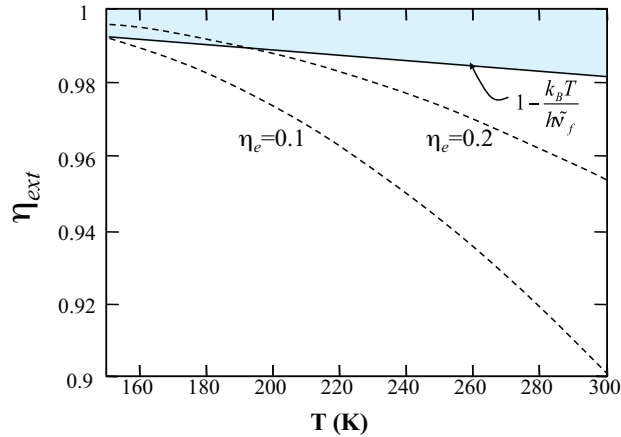
$$\bar{\eta}_{ext} = \eta_{ext} - \frac{\alpha_b(1-\eta_e)}{\bar{\alpha}_f \eta_e} > \frac{\nu}{\nu_f} + \frac{\alpha_b}{\alpha(\nu)} . \qquad (29)$$

The above inequality emphasizes the critical role of α_b in achieving net laser cooling. The quantity $\bar{\eta}_{ext}$ can be measured accurately, so Eq. (28) defines the minimum value of EQE for a given background absorption provided $\alpha(\nu)$

is known. The absorption $\alpha(\nu)$ drops sharply for energies considerably below the bandgap, which means this inequality may never be satisfied for any wavelength if α_b is too large. To quantify this argument, we need to know the band-tail absorption accurately. The nature of the band tail states and their dependence on the impurity type and concentration make the reported experimental values very sample-specific. Most theoretical calculations are accurate only for above and near the bandgap wavelengths. It is best to approach the problem experimentally with absorption and luminescence data that allow accurate estimates of the required EQE using Eq. (9). Starting with the measured low-density photoluminescence (PL) spectrum on a high quality sample, we obtain absorption spectra $\alpha(\nu)$ using the KMS relations of Eq. (13). The low density approximation reduces the occupation factor to a simple Boltzmann factor, $\exp(-h\nu/k_B T)$, where we ignore possible band-filling (saturation) effects in the band-tail. Using Eq. (9), the minimum required η_{ext} can be estimated as a function of $h\nu$ for various values of α_b, as depicted in Fig. 9. Here we assume an extraction efficiency η_e=0.1 which is typical of GaAs on a ZnS dome structure [15, 68]

Fig. 9 indicates that the required EQE for cooling becomes more demanding as the temperature is lowered which is essentially a consequence of diminishing phonon population at low temperatures. This result mirrors the situation in the rare-earth doped materials. Semiconductors, however, have the fortunate property that their EQE increases with decreasing temperature. The loss terms (A and C coefficients) decrease while the radiative rate (B coefficient) increases inversely with lattice temperature. Using the accepted scaling for C(T)∝exp(-β(300/T-1)) with $\beta \approx$2.4 for GaAs [55,69], taking $B \propto T^{-3/2}$ [59,70], keeping $h\tilde{\nu}_f/h\nu - 1 \approx k_B T/E_g$, and ignoring parasitic losses and the small temperature dependence of the band-gap energy, we obtain for the break-even nonradiative decay rate

$$\frac{A_0(T)}{A_0(300)} \approx \left(\frac{300}{T}\right) \exp\left(\frac{\beta(300-T)}{T}\right) . \qquad (30)$$
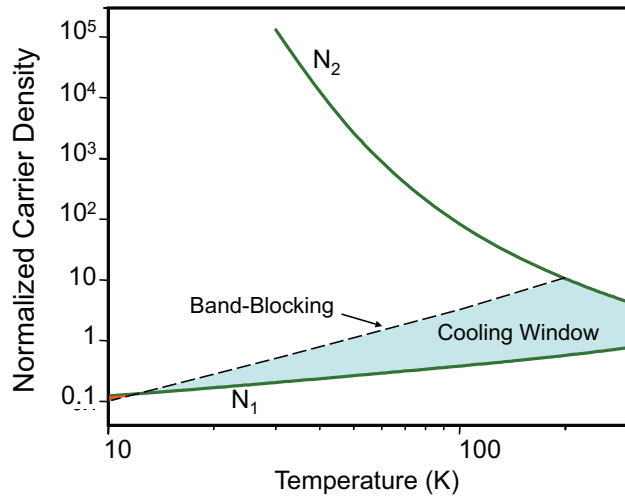
Laser & Photon. Rev. **3**, No. 1–2 (2009)

Laser & Photonics
Reviews

77

Figure 10 (online color at: www.lpr-journal.org) The required external quantum efficiency (EQE) as a function of temperature for GaAs under typical parameters.

Figure 11 (online color at: www.lpr-journal.org) The upper carrier density N_2, given by Eq. (26) is seen to be unattainable in GaAs due to band-blocking as temperature is lowered below 200 K. The middle (dashed) line represents the calculated density at which the band-tail absorption at $h\nu = h\nu_f - k_B T$ completely saturates (i.e. $\alpha(N)=0$, Eq. (10)). This is a worst case scenario for which the nonradiative recombination rate is assumed to be constant with temperature.

At $T = 150$ K, for example, the break-even lifetime is lowered by ~ 40 times compared with the room temperature ($T = 300$ K) condition. This is visualized by plotting η_{ext} versus T as is shown in Fig. 10 for two values of η_e. This range of values of η_e corresponds to a GaAs structure bonded to a high refractive index dome of ZnS or ZnSe [15, 68]. The solid red line indicates the break-even condition described by Eq. (2). This condition together with the fact that A (typically dominated by surface recombination) increases with temperature [70–72], makes the low temperature observation of laser cooling more favorable even though the overall efficiency ($\approx k_B T/E_g$) decreases. The reduction in cooling efficiency is effectively due to the reduction of the electron-phonon absorption probability at lower temperatures. In particular, the population of LO phonons with a corresponding reduction of the exciton linewidth Γ [59]:

$$\Gamma(T) = \Gamma_0 + \sigma T + \gamma N_{\text{LO}}(T) \tag{31}$$

where Γ_0 is due to impurities and inhomogeneous broadening, σ accounts for the contribution of acoustic phonons, and γ is the coefficient of LO-phonon scattering with N_{LO} (T) denoting the corresponding Bose-Einstein phonon distribution. For the exciton densities involved, we can ignore possible broadening due to exciton-exciton scattering [73]. As the lattice temperature approaches 10 K, the acoustic phonon contribution begins to dominate. At such low temperatures, however, the exciton-phonon scattering rate ($\approx \Gamma$) becomes comparable to the radiative recombination rate (BN^2) and consequently cold exciton recombination occurs before complete thermalization with the lattice. Similar processes, related to premature hot exciton recombination, have also hindered experimental observation of Bose-Einstein condensation in semiconductors. This problem is significantly alleviated by employing quantum confined systems where σ is enhanced by nearly 3 orders of magnitude. This relaxes wave-vector conserva-

tion along the confinement directions [74]. Enhanced cooling in quantum confined systems may allow operation at temperatures < 10 K.

Another issue of concern is absorption saturation (band-blocking) and many-body interactions. Band-blocking may be a limiting factor for long wavelength excitation where the low density of states gives rise to a stronger bleaching of the interband absorption. It is therefore necessary to have a good understanding of the absorption and emission spectra and its dynamic nonlinearities.

Theoretical models exist that deal with absorption spectra of semiconductor structures under various carrier densities and lattice temperatures. With different levels of complexity, there are theoretical calculations for 2D and 3D systems that deal with such many-body processes under dense e-h excitation [75–78]. Recently, a rigorous microscopic theory for absorption and luminescence in bulk semiconductors that includes the effects of electron-hole (e-h) plasma density as well as excitonic correlations has been introduced under the quasi-thermal equilibrium approximation [47, 79]. The reader is referred to the above sources for the details. Here, we use a simple model to estimate the effect of band-blocking on achieving the carrier densities of Eq. (26) for GaAs. Using the electron-hole density of states corresponding to a simple two-parabolic band model, we calculate the carrier density at which the occupation factor $\{f_v - f_c\}$ vanishes at $h\nu = h\nu_f - k_B T$. The result is depicted in Fig. 11 where this blocking density is contrasted with N_1 and N_2 of Eq. (26) evaluated using a constant A coefficient, and a temperature dependent B and

C coefficient used earlier. It is seen that band-blocking tends to reduce the cooling density window at $T < 200\,\text{K}$, and that cooling densities become unattainable at $T \approx 10\,\text{K}$. The simple model overestimates band-blocking effects, but qualitatively agrees with the more rigorous microscopic theory [47, 79]. Most recently, Khurgin has presented a thorough analysis of the phonon-assisted band-tail states and the role of band-blocking using a density-matrix approach [52]. In that context, he points out the significance of the excitation wavelength in the presence of band-blocking (saturation) which tends to diminish the cooling efficiency predominantly for $T \leqslant 100\,\text{K}$ [52].

Experimental work on optical refrigeration in semiconductors:

The first thorough experimental effort was reported by the University of Colorado [46]. No net cooling was achieved, despite realization of an impressive external quantum efficiency of 96% in GaAs. These experiments used a high quality GaAs heterostructure optically-contacted to a ZnSe dome structure for enhanced luminescence extraction. A report of local cooling in AlGaAs quantum wells by a European consortium [53] was later attributed to misinterpretation of spectra caused by Coulomb screening of the excitons [80]. Fig. 7b displays anti-Stokes luminescence in a GaAs heterostructure where excitation at λ=890 nm produces broadband luminescence with a mean wavelength of $\lambda_f \approx 860\,\text{nm}$. Each luminescent photon carries away about 40 meV more energy than an absorbed photon, so one might expect cooling. Why then have we not been able to observe laser cooling in this material or any semiconductor? To answer this question we have to revisit the cooling condition of Eq. (2) where strict requirements on EQE and background absorption are yet to be met. As discussed earlier, currently GaAs appears to be most promising due to the mature growth technology and record quantum efficiency. There are, however, challenges that must be overcome to achieve the break-even cooling condition: (a) reduce the surface recombination rate A, (b) reduce the parasitic background absorption α_b, and (c) enhance the luminescence extraction efficiency η_e. Issues (a) and (b) involve material preparation and both concern high purity growth using advance epitaxial methods. Condition (c), on the other hand, is a light management and device engineering challenge that deals with luminescence extraction from semiconductors having high index of refraction. Total internal reflection causes the majority of spontaneous emission to get trapped and re-absorbed. A similar problem limits the efficiency of light emitting diodes (LEDs).

Various methods have been devised to remedy this problem for LEDs but not all are applicable to laser cooling. For example, photon recycling in thin textured or in photonic bandgap structures can substantially enhance the luminescence extraction but at the price of redshifting the luminescence as described by Eq. 15 [15]. Index matched dome
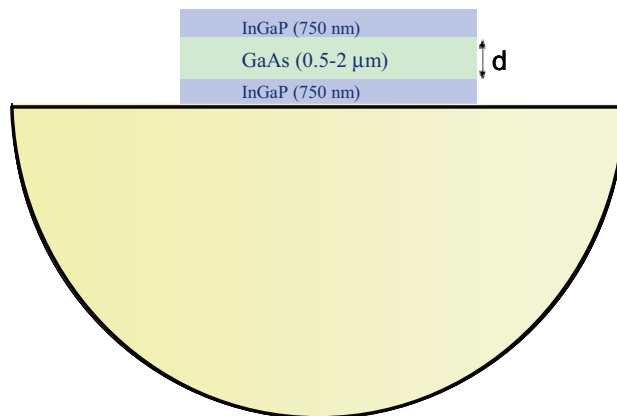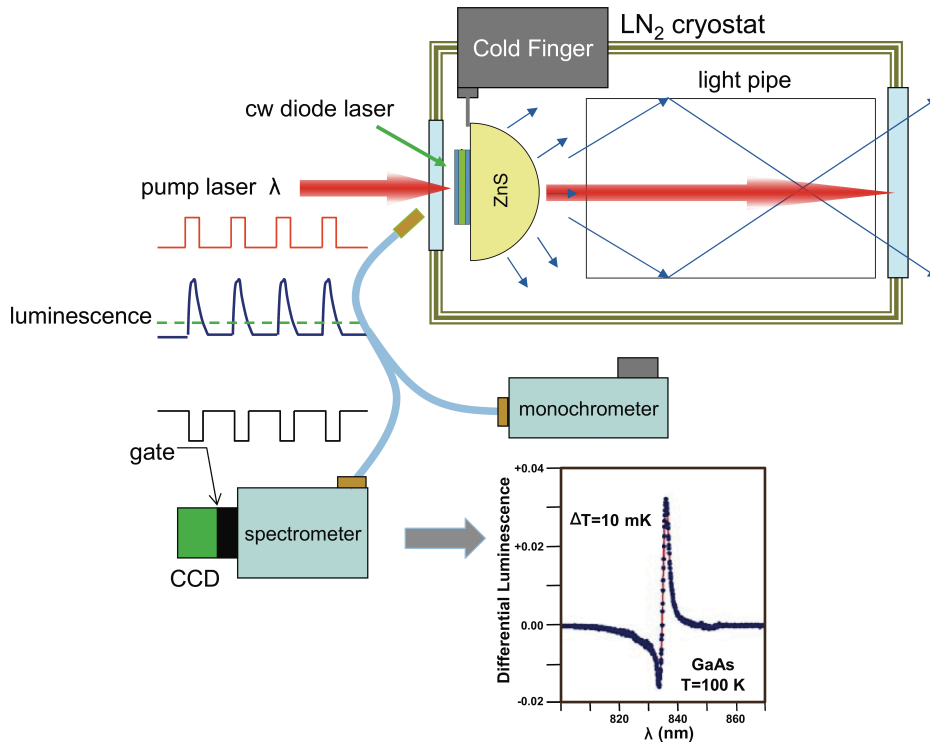

Figure 12 (online color at: www.lpr-journal.org) The GaAs/ GaInP double heterostructure is bonded to a nearly index-matched dome (ZnS or ZnSe) to enhance its luminescence extraction.

lenses have been exploited for LED's and can be used for laser cooling as well [46] provided the dome material does not introduce unacceptable levels of parasitic absorption. This requirement narrows the dome materials for GaAs to nearly index-matched ZnSe and ZnS due to their currently available high purity grade [81]. GaP substrates or domes can provide a higher η_e due to a better index matching to GaAs, but currently available materials produce unacceptable levels of parasitic absorption [81]. Another method for improving η_e makes use of nanometer dimension vacuum gaps (nanogap) as will be briefly discussed [6].

Highly controlled epitaxial growth techniques such as metal organic chemical vapor deposition (MOCVD) can produce very low surface recombination rates ($A < 10^4\,\text{sec}^{-1}$). This involves a double heterostructure of GaAs/GaInP as shown in Fig. 12 where the lattice-matched cladding layers provide surface passivation as well as carrier confinement. To deal with extraction efficiency, geometric coupling schemes such as nearly index-matched dome lenses (also shown in Fig. 12) have been employed to enhance η_e to 15%-20%. The double heterostructures are lithographically patterned into ≈ 1 mm diameter disks, lifted off from their parent GaAs substrates, and then van der-Waals bonded to a ZnS dome. The EQE of each sample is measured using the technique of fractional heating [46, 68] at various temperatures and laser pump powers.

The experimental setup is shown in Fig. 13. The pump laser is CW Ti:sapphire laser producing up to 4.5 W tunable in the wavelength range 750–900 nm. This laser is pumped by an 18 W laser at 532 nm (Verdi, Coherent Inc.). In the fractional heating experiment, the laser is tuned around the mean luminescence wavelength while the temperature ΔT of the sample is measured. According to analysis described earlier, the temperate change in the sample is proportional to the net power deposited which can be written as:

$$\Delta T(\lambda) = \kappa^{-1} P_{\text{abs}}(\lambda)\left(1 - \bar{\eta}_{\text{ext}}\eta_{\text{abs}}\frac{\lambda}{\lambda_f}\right) \quad (32)$$

Laser & Photon. Rev. **3**, No. 1–2 (2009)

Laser & Photonics Reviews 79

Figure 13 (online color at: www.lpr-journal.org) Experimental setup for measuring the external quantum efficiency (EQE or η_{ext}) at various lattice temperatures in GaAs/GaInP double heterostructures. A tunable cw laser (Ti:sapphire, 4.5 W) excites a constant density of electron-hole pairs as the pump is tuned near the band edge. This is done by keeping the luminescence intensity (within a certain spectral band) constant using the monochrometer. After recombination is complete, the temperature change of the sample is measured using differential luminescence thermometry (DLT) where the spectral shift of the low density luminescence spectrum induced by a weak cw laser diode is monitored using the gated spectrometer. The inset figure shows a typical DLT signal for $\Delta T = 10\,\text{mK}$ in GaAs at $T = 100\,\text{K}$.

where κ is the total thermal conductance (W/K) of the system positioned in an optical cryostat. During the experiment, the absorbed power is kept constant: the pump laser is tuned and its power adjusted to keep the luminescence (or a fixed spectral portion of it) constant. This is shown in Fig. 13 where a monochrometer is used to monitor the spectral portion of luminescence that does not overlap with the pump wavelength. The temperature change is monitored using a non-contact method called differential luminescence thermometry (DLT) that was developed for this purpose [68]. DLT exploits the temperature dependence of the luminescence resulting from the bandgap shift and broadening. High temperature sensitivity is obtained by monitoring the differential spectrum before and after pump irradiation. To avoid complications caused by high carrier density [80], low-density luminescence spectra induced by a weak diode laser generate the DLT signals. This is performed by modulating the pump laser with a mechanical chopper while synchronously gating a CCD camera on the spectrometer. This assures that the DLT spectra are recorded when the pump laser is blocked and after the high-density luminescence has decayed. DLT signals are obtained by normalizing the signal and reference spectra before subtraction. The resulting differential signal is a peak-valley or valley-peak feature depending on the sign of ΔT which is calibrated in situ before an experiment. This method has exhibited a temperature resolution better than 1 mK [68].

Returning to Eq. (32) it is evident that by keeping $P_{\text{abs}}(\lambda)$ constant, the measured ΔT versus λ follows the wavelength dependence of the cooling (or heating) effi-

ciency represented by the term in the bracket. At short wavelengths ($\lambda < \lambda_f$) where $\alpha(\lambda)$ is large, η_{abs} can be taken as unity for moderate to high purity samples, and the fractional heating data follows $\Delta T(\lambda) \propto (1 - \bar{\eta}_{\text{ext}}\lambda/\lambda_f)$ which is a straight line. Currently available samples do not possess sufficient purity to make this term negative, i.e. net cooling. When the pump wavelength λ is tuned close to λ_f, α_{abs} tends to degrade, thus preventing net cooling. Extrapolation of the short wavelength data can be used to obtain a "zero-crossing wavelength" λ_c from which $\bar{\eta}_{\text{ext}} = \lambda_f/\lambda_c$ can be deduced. Recall that $\eta_{\text{ext}} > \bar{\eta}_{\text{ext}}$ and thus we obtain a lower limit on EQE. When parasitic absorption of luminescence can be ignored then $\eta_{\text{ext}} \approx \bar{\eta}_{\text{ext}}$. In the following analysis of the experimental data, we refer to this lower limit measured by fractional heating technique as the EQE. Fig. 14a shows the measured EQE for various thicknesses of the GaAs layer at room temperature. The optimum GaAs thickness is found to be about 1 µm, determined by balancing excessive luminescence re-absorption for thicker layers with dominant surface recombination for thinner layers. [55, 82]. The measured temperature dependence of EQE is depicted in Fig. 14b, which is in qualitative agreement with the earlier analysis. Enhancement is observed as the temperature is lowered, reaching a record 99% at 100 K.

The fractional heating data leading to 99% EQE is shown in Fig. 15. We note the increase in temperature at longer wavelengths due to parasitic absorption. Knowing the absorption of GaAs, the data is fitted with a constant background $\alpha_b \approx 10\,\text{cm}^{-1}$ assuming it occurs entirely in the 1 µm thick GaAs layer. The experiment measures $\bar{\eta}_{\text{ext}}$ which means the unmodified EQE (η_{ext}) can be even larger.
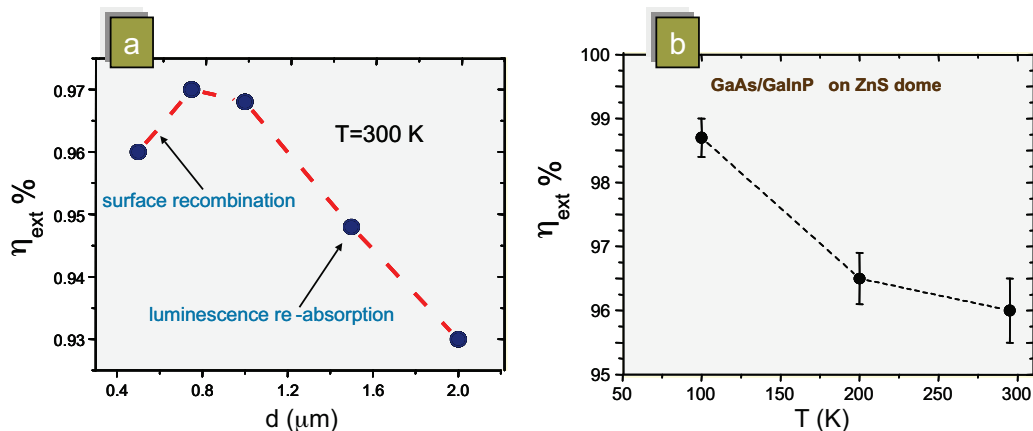
Figure 14 (online color at: www.lpr-journal.org) External quantum efficiency (EQE) measured with (a) a bonded sample of various GaAs thicknesses with the GaInP layers thickness fixed at 0.5 μm and $T = 300$ K, and (b) measured EQE versus lattice temperature for a GaAs thickness of 1 μm.
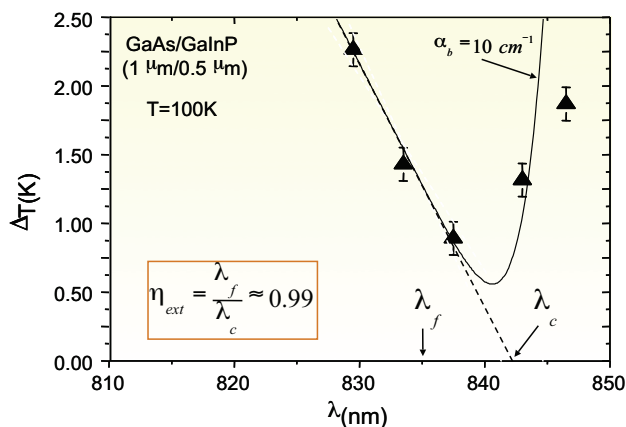
Figure 15 (online color at: www.lpr-journal.org) Fractional heating of 1 μm thick GaAs sample as a function of excitation wavelength for a fixed (optimum) electron-hole density at starting temperature of 100 K. The extrapolation of short wavelength data determines the zero-crossing wavelength from which a record EQE of ∼99% is measured. Excitation at longer wavelengths causes heating due to background parasitic absorption. [6, 68].

The average absorption coefficient ($\bar{\alpha}_f \approx 4000\,\text{cm}^{-1}$) allows us to estimate an upper limit for α_b inside the double heterostructure. Even if $\eta_{\text{ext}} = 1$, attaining $\bar{\eta}_{\text{ext}} = 99\%$, requires that $\alpha_b < \frac{(1-\bar{\eta}_{\text{ext}})}{(1-\eta_e)/\eta_e}\bar{\alpha}_f \approx 4\,\text{cm}^{-1}$ assuming $\eta_e \approx 0.1$. The value of $\alpha_b = 10\,\text{cm}^{-1}$ that was used to fit the data in Fig. 15 may have contributions from sources outside the double heterostructure such as dome or cold-finger contacts.

Experiments show that even though external quantum efficiency is adequate for achieving net laser cooling, the purity of the samples is not yet sufficient. Efforts are underway to address this material problem. Researchers at the National Renewable Energy Laboratory are using highly controlled MOCVD growth and scientists at the University of New Mexico are exploring aluminum-free GaAs heterostructure growth using phosphorous molecular beam epitaxy (MBE).

Methods to enhance η_{ext} by improving luminescence extraction efficiency are being explored as well. A novel method based on the frustrated total internal reflection across a vacuum "nano-gap" is being developed at the University of New Mexico [17, 83, 84]. In this scheme, the luminescence photons tunnel through the gap into the absorber region. The vacuum nano-gap maintains a thermal barrier between the heterostructure and the absorber/heat sink. The cooling heterostructure and luminescence absorber are thus optically contacted but thermally insulated. Calculations show that a gap spacing of < 25 nm has higher extraction efficiency than the dome structure (GaAs on ZnS or ZnSe) and preliminary fabrication of such structures show promising results. Using a multi step photolithographic process, a Si-based nano-gap with 50 nm spacing supported by posts have been monolithically fabricated as depicted in Fig. 16 [83]. Recently, we have fabricated GaAs nano-gap structures that will be integrated with a high quality GaAs heterostructure to investigate their performance in cooling experiments.

5. Future outlook

Optical refrigeration has advanced from basic principles to a promising technology. Cooling of rare-earth based materials is approaching cryogenic operation. In semiconductors, much progress has been made in achieving high external quantum efficiency. With advanced heterostructure growth and novel device fabrication currently underway, cooling will soon be attainable. In the coming years, optical refrigeration will be useful in applications such as satellite instrumentation and small sensors, where compactness,

Laser & Photon. Rev. **3**, No. 1–2 (2009)

Laser & Photonics
Reviews

81
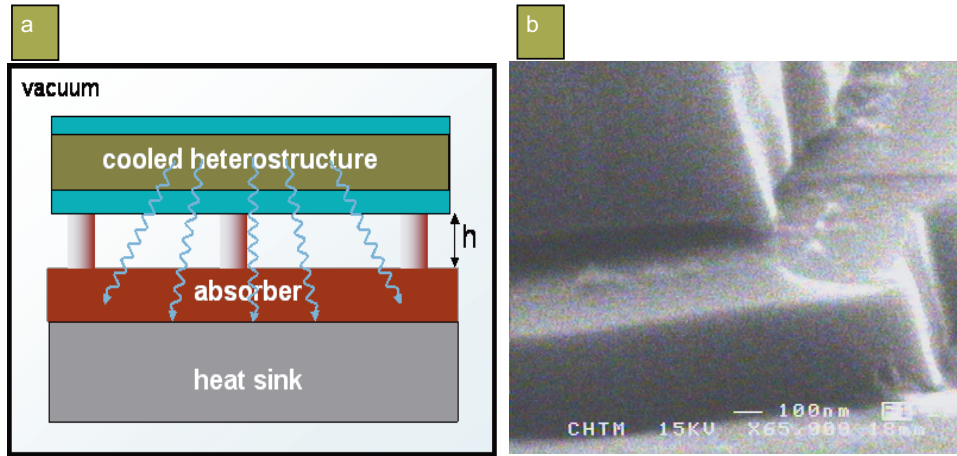
Figure 16 (online color at: www.lpr-journal.org) (a) A vacuum "nano-gap" structure where the heterostructure is situated (e.g. supported by posts) at a sub-wavelength distance from an absorber. Luminescence photons will escape into the absorber via frustrated total internal reflection (photon tunneling) while the gap provides a thermal barrier. (b) The SEM micrographs of a preliminary nanogap structure (with 50 nm spacing) fabricated using a multi-step photolithographic technique [83].

ruggedness, and the lack of vibrations are important. Optical refrigeration is well suited for space-borne applications since it has no moving parts and can be designed for long operational lifetimes. Additionally, the cooling element is not electrically powered so it will not interfere with the electronics being cooled. One can envision optical refrigerators being directly integrated with infrared sensors for thermal imaging of the earth and of astrophysical objects. In terrestrial applications, small size and reliability make optical refrigerators attractive for use with high-temperature superconductor sensors and electronics. Optical refrigeration could enable compact SQUID magnetometers for geophysical and biomedical sensing and may be a critical component in the production commercial electronics incorporating fast and efficient superconducting components.

6. Appendix:
Photon waste recycling and the carnot limit

Many applications will be possible if the basic efficiency of optical refrigerators $\sim k_{\rm B}T/h\nu$ can be improved. This efficiency limit assumes all fluorescence photons are absorbed by a heat sink and thus wasted. This is depicted diagrammatically in Fig. 17a. One expects improved overall efficiency if fluorescence photons are recycled with photovoltaic (PV) elements to convert them into electricity [85]. This recovered energy can be used to drive laser diodes (LD) at the pump photon energy $h\nu$. This process is diagrammed in Fig. 17b.

Deriving the new cooling efficiency is then straightforward: For the same cooling power (P_c) as in the open loop system, the required laser power in the photon-waste recycled system is lowered by the amount generated by recycling: $\eta_{\rm PV}\eta_L P_f$ where P_f is the luminescence power
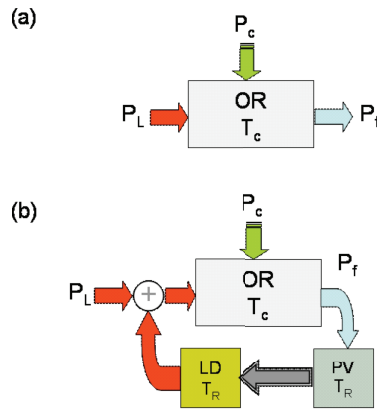
Figure 17 (online color at: www.lpr-journal.org) Diagrammatical representation of (a) an open loop optical refrigerator (OR) and (b) a closed loop system in which the luminescence (photon waste) recycling is performed using photovoltaic (PV) followed by a laser diode (LD) both at temperature T_R.

and η_{PV} and η_L are power efficiencies of the photovoltaic and the laser diode, respectively. The enhanced cooling efficiency $\bar{\eta}_c$ is then obtained as

$$\bar{\eta}_c = \frac{\eta_c}{1 - \eta_{PV}\eta_L(1 - \eta_c)} \quad , \qquad (33)$$

where the "old" or open loop cooling efficiency $\eta_c = 1 - P_f/P_L$, as before. It is useful to investigate what limits this new efficiency. Assuming η_c is given by its quantum limit of $h\nu_f/h\nu - 1$, we take $h\nu = h\nu_f - mk_B T_c$ where m if of the order of unity and T_c is the temperature of the solid-state coolant. This leads to $\eta_c = mk_B T_c/h\nu_f \approx mk_B T_c/E_{\rm g}$ where $E_{\rm g}$ is the energy gap of the transition. The obvious choice for the photovoltaic and laser diode system will be a semiconductor with energy gap very close to $E_{\rm g}$. Assuming both are at a reservoir temperature of T_R, it is not unreasonable to take their conversion efficiency to be $\eta_{PV} = 1 - pk_B T_R/E_{\rm g}$ and $\eta_L = 1 - qk_B T_R/E_{\rm g}$, respectively. Current devices reach efficiencies that correspond to $p \approx q \approx 30$–50, so one expects they will be limited by

$p \approx q \approx 1$. In such a limit one writes Eq. (33) as:

$$\bar{\eta}_c = \frac{T_C}{T_C + \left(\frac{p+q}{m}\right) T_R} \qquad (34)$$

We note that thermodynamic analysis require that $p + q \geqslant m \approx 1$. With $p + q = m \approx 1$, one obtains the Carnot limit of $T_C/(T_C + T_R)$. Expected technological advances in photovoltaic and laser diode devices will enable efficiencies approaching that corresponding to $p \approx q \approx 1$, hence the ultimate efficiency of the optical refrigerator will be given by its Carnot limit.

Mansoor Sheik-Bahae is professor of Physics and Astronomy and chair of Optical Science and Engineering at the University of New Mexico (UNM), Albuquerque NM (USA). He graduated from the State University of New York (Buffalo), and subsequently spent 7 years as a research professor at CREOL-University of Central Florida before joining UNM in 1994 where he currently heads the Consortium for Laser Cooling of Solids. Professor Sheik-Bahae has authored more than 200 scientific papers in nonlinear optics, ultrafast phenomena and solid-state laser cooling, with more than 4000 citations to his work. He is a fellow of Optical Society of America.

Richard Epstein is a Laboratory Fellow at Los Alamos National Laboratory (LANL) in New Mexico. He was an undergraduate in Engineering Physics at Cornell University and received his Ph.D. in Applied Physics from Stanford University. He then did research at the University of Texas at Austin, Harvard University and Nordita in Copenhagen, before taking his present position. Dr. Epstein has published over 150 papers in theoretical astrophysics, satellite instrumentation and applied physics. He leads the effort in laser cooling of solids at LANL. He is a fellow of Optical Society of America.

References

[1] S. Chu, C. Cohen-Tannoudji, and W. D. Philips, Nobel Prize in Physics 1997 for development of methods to cool and trap atoms with laser light.

[2] E. A. Cornell, W. Ketterle, and C. E. Weiman, Nobel Prize in Physics 2001 for the achievement of Bose-Einstein condensation in dilute gases of alkali atoms, and for early fundamental studies of the properties of the condensates.

[3] P. Pringsheim, Zwei Bemerkungen über den Unterschied von Lumineszenz- und Temperaturstrahlung, Z. Phys. **57**, 739 (1929).

[4] B. C. Edwards, M. I. Buchwald, and R. I. Epstein, Development of the Los-Alamos Solid-State Optical Refrigerator, Rev. Sci. Instrum. **69**, 2050–2055 (1998).

[5] B. C. Edwards, J. E. Anderson, R. I. Epstein, G. L. Mills, and A. J. Mord, Demonstration of a solid-state optical cooler: An approach to cryogenic refrigeration, J. Appl. Phys. **86**, 6489–6493 (1999).

[6] M. Sheik-Bahae and R. I. Epstein, Optical refrigeration, Nature Photonics **1**, 693–699 (2007).

[7] G. Mills and A. Mord, Performance modeling of optical refrigerators, Cryogenics **46**, 176–182 (2005).

[8] S. R. Bowman, Lasers without internal heat generation, IEEE J. Quantum Electron. **35**, 115–122 (1999).

[9] S. R. Bowman and C. E. Mungan, New materials for optical cooling, Appl. Phys. B, Lasers Opt. **71**, 807–811 (2000).

[10] L. Landau, On the thermodynamics of photoluminescence, J. Phys. (Russia) **10**, 503 (1946).

[11] A. Kastler, J. Phys. Radium **11**, 255–265 (1950).

[12] T. Kushida and J. E. Geusic, Optical refrigeration in Nd-doped yttrium aluminum garnet, Phys. Rev. Lett. **21**, 1172–1175 (1968).

[13] S. Yatsiv, Anti-Stokes fluorescence as a cooling process, in: Advances in Quantum Electronics, edited by J. R. Singer (Columbia University, New York, 1961), pp. 200–213.

[14] R. I. Epstein, M. I. Buchwald, B. C. Edwards, T. R. Gosnell, and C. E. Mungan, Observation of Laser-Induced Fluorescent Cooling of a Solid, Nature **377**, 500–503 (1995).

[15] M. Sheik-Bahae and R. I. Epstein, Can laser light cool semiconductors?, Phys. Rev. Lett. **92**, 247403 (2004).

[16] P. Asbeck, Self-absorption effects on radiative lifetime in GaAs-GaAlAs double heterostructures, J. Appl. Phys. **48**, 820–822 (1977).

[17] M. Sheik-Bahae, B. Imangholi, M. P. Hasselbeck, R. I. Epstein, and S. Kurtz, Advances in laser cooling of semiconductors, in: Proceedings of the SPIE: Physics and Simulation of Optoelectronic Devices XIV, Vol. 6115, edited by M. Osinski, F. Henneberger, and Y. Arakawa (SPIE, San Jose, CA, 2006), p. 611518.

[18] D. Emin, Laser cooling via excitation of localized electrons, Phys. Rev. B, Cond. Matter Mater. Phys. **76**, 024301 (2007).

[19] C. E. Mungan, M. I. Buchwald, B. C. Edwards, R. I. Epstein, and T. R. Gosnell, Laser cooling of a solid by 16 K starting from room-temperature, Phys. Rev. Lett. **78**, 1030–1033 (1997).

[20] X. Luo, M. D. Eisaman, and T. R. Gosnell, Laser cooling of a solid by 21 K starting from room temperature, Opt. Lett. **23**, 639–641 (1998).

[21] T. R. Gosnell, Laser cooling of a solid by 65 K starting from room temperature, Opt. Lett. **24**, 1041–1043 (1999).

[22] J. Thiede, J. Distel, S. R. Greenfield, and R. I. Epstein, Cooling to 208 K by optical refrigeration, Appl. Phys. Lett. **86**, 154107 (2005).

[23] A. Rayner, M. E. J. Friese, A. G. Truscott, N. R. Heckenberg, and H. Rubinsztein-Dunlop, Laser cooling of a

Laser & Photon. Rev. **3**, No. 1–2 (2009)

Laser & Photonics
Reviews

83

solid from ambient temperature, J. Mod. Opt. **48**, 103–114 (2001).

[24] B. Heeg, M. D. Stone, A. Khizhnyak, G. Rumbles, G. Mills, and P. A. DeBarber, Experimental demonstration of intracavity solid-state laser cooling of Yb3+: ZrF4-BaF2-LaF3-AlF3-NaF glass, Phys. Rev. A **70**, 021401 (2004).

[25] J. R. Fernandez, A. Mendioroz, R. Balda, M. Voda, M. Al-Saleh, A. J. Garcia-Adeva, J.-L. Adam, and J. Lucas, Origin of laser-induced internal cooling of Yb[sup 3 +]-doped systems, in: Rare-Earth-Doped Materials and Devices VI, Vol. 4645, edited by S. Jiang and R. W. Keys (SPIE, San Jose, CA, 2002), pp. 135–147.

[26] J. Fernandez, A. Mendioroz, A. J. Garcia, R. Balda, and J. L. Adam, Anti-Stokes laser-induced internal cooling of Yb3+-doped glasses, Phys. Rev. B **62**, 3213–3217 (2000).

[27] R. I. Epstein, J. J. Brown, B. C. Edwards, and A. Gibbs, Measurements of optical refrigeration in ytterbium-doped crystals, J. Appl. Phys. **90**, 4815–4819 (2001).

[28] A. Mendioroz, J. Fernandez, M. Voda, M. Al-Saleh, R. Balda, and A. Garcia-Adeva, Anti-stokes laser cooling in Yb3+-doped KPb2Cl5 crystal, Opt. Lett. **27**, 1525–1527 (2002).

[29] S. Bigotta, D. Parisi, L. Bonelli, A. Toncelli, A. Di Lieto, and M. Tonelli, Laser cooling of Yb3+-doped BaY2F8 single crystal, Opt. Mater. **28**, 1321–1324 (2006).

[30] S. Bigotta, D. Parisi, L. Bonelli, A. Toncelli, M. Tonelli, and A. Di Lieto, Spectroscopic and laser cooling results on Yb3+-doped BaY2F8 single crystal, J. Appl. Phys. **100**, 013109 (2006).

[31] W. Patterson, S. Bigotta, M. Sheik-Bahae, D. Parisi, M. Tonelli, and R. Epstein, Anti-Stokes luminescence cooling of Tm3+doped BaY2F8, Opt. Express **16**, 1704–1710 (2008).

[32] S. Bigotta, A. D. Lieto, D. Parisi, A. Toncelli, and M. Tonelli, Single Fluoride Crystals as Materials for Laser Cooling Applications, presented at Laser Cooling of Solids, 2007.

[33] D. Seletskiy, M. P. Hasselbeck, M. Sheik-Bahae, R. I. Epstein, S. Bigotta, and M. Tonelli, Cooling of Yb:YLF Using Cavity Enhanced Resonant Absorption, presented at Laser Refrigeration of Solids, San Jose, CA, USA, 2008.

[34] C. W. Hoyt, M. Sheik-Bahae, R. I. Epstein, B. C. Edwards, and J. E. Anderson, Observation of anti-Stokes fluorescence cooling in thulium-doped glass, Phys. Rev. Lett. **85**, 3600–3603 (2000).

[35] C. Hoyt, M. Hasselbeck, M. Sheik-Bahae, R. Epstein, S. Greenfield, J. Thiede, J. Distel, and J. Valencia, Advances in laser cooling of thulium-doped glass, J. Opt. Soc. Am. B **20**, 1066–1074 (2003).

[36] J. Fernandez, A. J. Garcia-Adeva, and R. Balda, Anti-Stokes laser cooling in bulk erbium-doped materials, Phys. Rev. Lett. **97**, 033001 (2006).

[37] A. J. Garcia-Adeva, R. Balda, and J. Fernandez, Anti-Stokes Laser Cooling in Erbium-Doped Low-Phonon Materials, in: Proceedings of the SPIE: Laser Cooling of Solids, Vol. 6461, edited by R. I. Epstein and M. Sheik-Bahae (SPIE, San Jose, CA, 2007), p. 646102-1.

[38] G. Lamouche, P. Lavallard, R. Suris, and R. Grousson, Low temperature laser cooling with a rare-earth doped glass, J. Appl. Phys. **84**, 509–516 (1998).

[39] M. P. Hehlen, R. I. Epstein, and H. Inoue, Model of laser cooling in the Yb3+-doped fluorozirconate glass ZBLAN, Phys. Rev. B **75**, 144302 (2007).

[40] C. W. Hoyt, Laser Cooling in Thulium-doped Solids, Ph. D. Thesis, University of New Mexico, 138 pages,2003

[41] D. Seletskiy, M. P. Hasselbeck, M. Sheik-Bahae, and R. I. Epstein, Laser Cooling using Cavity Enhanced Pump Absorption, in: Proceedings of the SPIE: Laser Cooling of Solids, Vol. 6461, edited by R. I. Epstein and M. Sheik-Bahae (SPIE, San Jose, CA, 2007), p. 646104.

[42] X. L. Ruan and M. Kaviany, Enhanced laser cooling of rare-earth-ion-doped nanocrystalline powders, Phys. Rev. B **73**, 155422 (2006).

[43] J. L. Clark and G. Rumbles, Laser cooling in the condensed-phase by frequency up-conversion, Phys. Rev. Lett. **76**, 2037–2040 (1996).

[44] A. N. Oraevsky, Cooling of semiconductors by laser radiation, J. Russ. Laser Res. **17**, 471–479 (1996).

[45] L. A. Rivlin and A. A. Zadernovsky, Laser cooling of semiconductors, Opt. Commun. **139**, 219–222 (1997).

[46] H. Gauck, T. H. Gfroerer, M. J. Renn, E. A. Cornell, and K. A. Bertness, External radiative quantum efficiency of 96% from a GaAs/GaInP heterostructure, Appl. Phys. A, Mater. Sci. Process. **64**, 143–147 (1997).

[47] G. Rupper, N. H. Kwong, and R. Binder, Large excitonic enhancement of optical refrigeration in semiconductors, Phys. Rev. Lett. **97**, 117401 (2006).

[48] D. H. Huang, T. Apostolova, P. M. Alsing, and D. A. Cardimona, Spatially selective laser cooling of carriers in semiconductor quantum wells, Phys. Rev. B **72**, 195308 (2005).

[49] J. Z. Li, Laser cooling of semiconductor quantum wells: Theoretical framework and strategy for deep optical refrigeration by luminescence upconversion, Phys. Rev. B **75**, 155315 (2007).

[50] G. Rupper, N. H. Kwong, and R. Binder, Optical refrigeration of GaAs: Theoretical study, Phys. Rev. B, Condens, Matter Mater. Phys. **76**, 245203 (2007).

[51] D. Huang and P. M. Alsing, Many-body effects on optical carrier cooling in intrinsic semiconductors at low lattice temperatures, Phys. Rev. B, Condens, Matter Mater. Phys. **78**, 035206 (2008).

[52] J. B. Khurgin, Role of bandtail states in laser cooling of semiconductors, Phys. Rev. B, Condens, Matter Mater. Phys. **77**, 235206 (2008).

[53] E. Finkeissen, M. Potemski, P. Wyder, L. Vina, and G. Weimann, Cooling of a semiconductor by luminescence up-conversion, Appl. Phys. Lett. **75**, 1258–1260 (1999).

[54] T. H. Gfroerer, E. A. Cornell, and M. W. Wanlass, Efficient directional spontaneous emission from an InGaAs/InP heterostructure with an integral parabolic reflector, J. Appl. Phys. **84**, 5360–5362 (1998).

[55] B. Imangholi, M. P. Hasselbeck, M. Sheik-Bahae, R. I. Epstein, and S. Kurtz, Effects of epitaxial lift-off on interface recombination and laser cooling in GaInP/GaAs heterostructures, Appl. Phys. Lett. **86**, 81104 (2005).

[56] S. Eshlaghi, W. Worthoff, A. D. Wieck, and D. Suter, Luminescence upconversion in GaAs quantum wells, Phys. Rev. B, Condens, Matter Mater. Phys. **77**, 245317 (2008).

[57] J. B. Khurgin, Surface plasmon-assisted laser cooling of solids, Phys. Rev. Lett. **98**, 177401 (2007).

[58] J. B. Khurgin, Band gap engineering for laser cooling of semiconductors, J. Appl. Phys. **100**, 113116 (2006).

[59] P. K. Basu, Theory of optical processes in semiconductors: bulk and microstructures (Oxford University Press, New York, 1997).

[60] J. I. Pankove, Optical processes in semiconductors (Prentice-Hall, Englewood Cliffs, N. J., 1971).

[61] M. Born and E. Wolf, Principles of optics: electromagnetic theory of propagation, interference and diffraction of light, 7th expanded ed. (Cambridge University Press, Cambridge, New York, 1999).

[62] W. van Roosbroeck and W. Shockley, Phys. Rev. **94**, 1558 (1954).

[63] S. L. Chuang, Physics of Optoelectronic Devices (Wiley, New York, 1995).

[64] J. Piprek, Semiconductor Optoelectronic Devices: Introduction to Physics and Simulation (Academic Press, Amsterdam, Boston, 2003).

[65] E. Yablonovitch, T. J. Gmitter, and R. Bhat, Inhibited and enhanced spontaneous emission from optically thin algaas gaas double heterostructures, Phys. Rev. Lett. **61**, 2546–2549 (1988).

[66] A. Haug, Free-carrier absorption in semiconductor-lasers, Semicond. Sci. Technol. **7**, 373–378 (1992).

[67] H. Yi, J. Diaz, B. Lane, and M. Razeghi, Optical losses of Al-free lasers for lambda=0.808 and 0.98 mu m, Appl. Phys. Lett. **69**, 2983–2985 (1996).

[68] B. Imangholi, Investigation of Laser Cooling in Semiconductors, Ph. D. Thesis, University of New Mexico (2006).

[69] G. P. Agrawal and N. K. Dutta, Long-Wavelength Semiconductor Lasers (Van Nostrand Reinhold, New York, 1986).

[70] G. W. Thooft and C. Vanopdorp, Temperature-dependence of interface recombination and radiative recombination in (Al, Ga)As heterostructures, Appl. Phys. Lett. **42**, 813–815 (1983).

[71] R. K. Ahrenkiel, J. M. Olson, D. J. Dunlavy, B. M. Keyes, and A. E. Kibbler, Recombination velocity of the Ga0.5In0.5P/GaAs interface, J. Vac. Sci. Technol. A, Vac. Surf. Films **8**, 3002–3005 (1990).

[72] J. M. Olson, R. K. Ahrenkiel, D. J. Dunlavy, B. Keyes, and A. E. Kibbler, Ultralow recombination velocity of the Ga0.5In0.5P/GaAs heterointerfaces, Appl. Phys. Lett. **55**, 1208–1210 (1989).

[73] A. C. Schaefer and D. G. Steel, Nonlinear optical response of the GaAs exciton polariton, Phys. Rev. Lett. **79**, 4870–4873 (1997).

[74] L. V. Butov, C. W. Lai, A. L. Ivanov, A. C. Gossard, and D. S. Chemla, Towards Bose-Einstein condensation of excitons in potential traps, Nature **417**, 47–52 (2002).

[75] L. Banyai and S. W. Koch, A simple theory for the effects of plasma screening on the optical-spectra of highly excited semiconductors, Z. Phys. B, Condens. Matter **63**, 283–291 (1986).

[76] H. Haug and S. W. Koch, Quantum Theory of the Optical and Electronic Properties of Semiconductors, 3rd ed. (World Scientific, Singapore, 1994).

[77] J. P. Lowenau, F. M. Reich, and E. Gornik, Many-body theory of room-temperature optical nonlinearities in bulk semiconductors, Phys. Rev. B, Condens. Matter **51**, 4159–4165 (1995).

[78] T. Meier and S. W. Koch, Coulomb correlation signatures in the excitonic optical nonlinearities of semiconductors, Semicond. Semimetals **67**, 231–313 (2001).

[79] G. Rupper, N. H. Kwong, and R. Binder, Optical refrigeration of GaAs: Theoretical study, Phys. Rev. B **76**, 245203 (2007).

[80] M. P. Hasselbeck, M. Sheik-Bahae, and R. I. Epstein, Effect of high carrier density on luminescence thermometry in semiconductors, in: Proceedings of the SPIE: Laser Cooling of Solids, Vol. 6461, edited by R. I. Epstein and M. Sheik-Bahae (SPIE, San Jose, CA, 2007), p. 646107.

[81] B. Imangholi, M. P. Hasselbeck, and M. Sheik-Bahae, Absorption spectra of wide-gap semiconductors in their transparency region, Opt. Commun. **227**, 337–341 (2003).

[82] K. R. Catchpole, K. L. Lin, P. Campbell, M. A. Green, A. W. Bett, and F. Dimroth, High external quantum efficiency of planar semiconductor structures, Semicond. Sci. Technol. **19**, 1232–1235 (2004).

[83] R. P. Martin, J. Velten, A. Stintz, K. J. Malloy, R. I. Epstein, M. Sheik-Bahae, M. P. Hasselbeck, B. Imangholi, S. T. P. Boyd, and T. M. Bauer, Nanogap experiments for laser cooling: a progress report, in: Proceedings of the SPIE: Laser Cooling of Solids, Vol. 6461, edited by R. I. Epstein and M. Sheik-Bahae (SPIE, San Jose, CA, 2007), p. 64610H.

[84] R. I. Epstein, B. C. Edwards, and M. Sheik-Bahae, Semiconductor-Based Optical Refrigerator, U. S. Patent No. 6,378,321,2002.

[85] B. C. Edwards, M. I. Buchwald, and R. I. Epstein, Optical Refrigerator using Reflectivity Tuned Dielectric Mirrors, U. S. Patent No. 6041610,2000.